THE ASTROPHYSICAL JOURNAL, 320:L27–L33, 1987 September 1

IRAS OBSERVATIONS OF SUPERNOVA REMNANTS: A COMPARISON BETWEEN THEIR INFRARED AND X-RAY COOLING RATES

ELI DWEK[1]
Laboratory for Astronomy and Solar Physics, NASA/Goddard Space Flight Center
ROBERT PETRE[1] AND ANDREW SZYMKOWIAK[1]
Laboratory for High Energy Astrophysics, NASA/Goddard Space Flight Center
AND
WALTER L. RICE
Jet Propulsion Laboratory, California Institute of Technology
Received 1986 June 30; accepted 1987 June 30

ABSTRACT

IRAS infrared observations of several Galactic supernova remnants (SNR), including the brightest X-ray remnants, reveal that infrared emission from collisionally heated dust is the dominant cooling mechanism during much of their lifetimes. We compare the infrared fluxes from selected Galactic SNR observed by *IRAS* with their existing X-ray fluxes to derive an infrared-to-X-ray flux ratio (hereafter referred to as the IRX ratio) for a variety of SNR. These include the relatively young remnants Cas A, Tycho, Kepler, SN 1006, RCW 86, and RCW 103; and the more evolved remnants IC 443, Puppis A, and the Cygnus Loop. The IRX ratio is a measure of the relative importance of remnant cooling by gas-grain collisions to its cooling by atomic processes, and for all the above remnants (with the possible exception of SN 1006 and RCW 103) we found that the IRX ratio is significantly greater than unity.

We also compare the observed IRX ratio to the theoretically derived ratio, which for a gas in collisional ionization equilibrium with a given dust-to-gas mass ratio depends only on the temperature of the shocked gas. Remnants with IRX ratios that deviate significantly from the predicted value are most likely encountering regions of the interstellar medium (ISM) that are different from that assumed in the model. These differences might reflect either inhomogeneities in the ISM or influences the supernova progenitor had upon the local medium. Infrared observations can therefore provide valuable information on the interaction of remnants with the ambient ISM.

Subject headings: infrared: sources — nebulae: supernova remnants — radiation mechanisms — X-rays: sources

I. INTRODUCTION

Theoretical calculations suggest that at temperatures above $\sim 10^6$ K, infrared cooling by gas-grain collisions dominates the cooling of a dusty astrophysical plasma (Spitzer 1968; Dalgarno and McCray 1972; Ostriker and Silk 1973; Burke and Silk 1974; Draine 1981; Dwek 1987). Since supernova remnants expand in a dusty interstellar medium (ISM), the presence of dust in the shocked gas can significantly affect their luminosity and to some extent their dynamical evolution (Silk and Burke 1974; Dwek 1981). The extent to which these theoretical calculations apply to observed supernova remnants is therefore a question of great astrophysical interest.

To compare the relative importance of remnant cooling by means of gas-grain collisions and atomic processes (these include free-free, free-bound, and bound-bound transitions) we define a quantity, IRX, to be the ratio between the infrared (IR) flux and the 0.2–4.0 keV X-ray flux from the remnant. This comparison is now possible as a result of the successful *Infrared Astronomical Satellite* (*IRAS*) 12, 25, 60, and 100 μm all-sky survey, which included the detection of many supernova remnants (Braun 1986*a*, *b*, 1987*a*; Arendt 1987). Since a significant fraction of the atomic cooling of the remnants is at X-ray wavelengths and dust cooling occurs at IR wavelengths, the IRX ratio is a measure of the relative importance of these two distinct cooling mechanisms. The actual IRX ratio in remnants can deviate significantly from the theoretically predicted value, and a combined study of the IRX ratio and the infrared morphology of supernova remnants can yield important information on their evolutionary stage and dynamical interaction with the ambient ISM. An observed IRX ratio in excess of the theoretically calculated value may indicate that the dust-to-gas mass ratio in the ambient ISM is above its average value, that a significant contribution to the IR flux is of nonthermal origin, or that most of the IR emission originates from dust that is not mixed with the X-ray emitting gas. On the other hand, an observed IRX ratio that is significantly smaller than the calculated value may indicate that the dust is depleted, or not well coupled to the hot gas.

[1]General Investigator with the NASA *IRAS* Extended Mission Program.

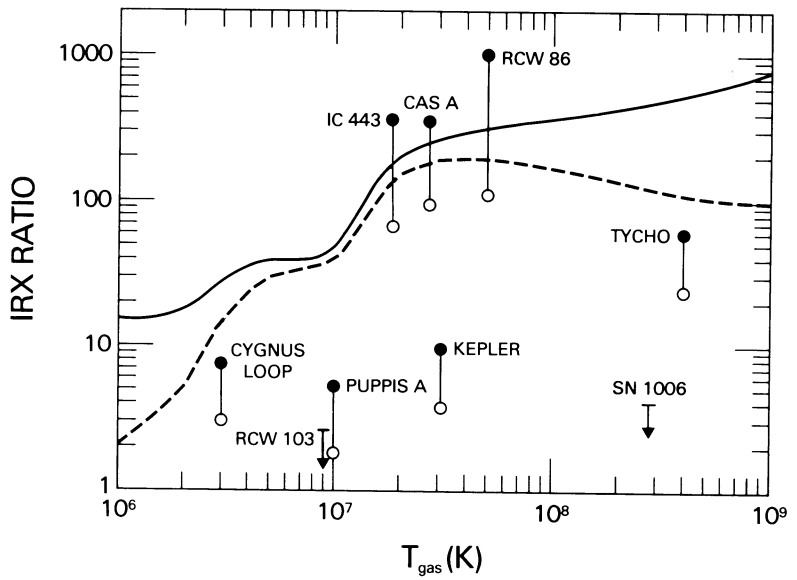

FIG. 1.—The infrared-to-atomic cooling ratio, defined as $\Lambda_d(T)/\Lambda(T)$ (eq. [1]), is plotted here as a function of plasma temperature, T (*dashed line*). The solid line represents the IRX ratio defined as $\Lambda_d(T)/\Lambda_{0.2-4.0}(T)$, the ratio of the infrared cooling to X-ray cooling in the 0.2–4.0 keV band. Estimates of the ratio of infrared to 0.2–4.0 keV band fluxes for several remnants are shown by the unfilled symbols. Where the authors of the original analyses of the X-ray images identified some of the X-ray flux as arising in shocked ejecta (Cas A and Tycho), the ratio was formed using only the X-ray flux attributed to shocked interstellar material. The "observed" ratios cannot be directly compared with the predicted curve, as the model neglects the enhancement of the X-ray fluxes caused by nonequilibrium ionization. The filled points represents an attempt to correct the "observed" ratios for this effect, to facilitate a comparison with the model. The procedures used for forming the "observed" ratios and the correction factors are described in the text.

In this *Letter* we present a comparison between the total IR and X-ray cooling rates of nine selected Galactic supernova remnants, deferring the analysis of their morphologies to separate papers. A qualitative comparison of the IR and X-ray emission from *IRAS* detected remnants in the Large Magellanic Cloud shows that infrared cooling dominates the atomic cooling by a factor of ~ 10 (Graham *et al.* 1987). We find that for all remnants discussed here (with the possible exception of SN 1006 and RCW 103) IR emission is the dominant cooling mechanism of the shocked gas. We first calculate (in § II) the dust-to-gas cooling ratio and the IRX ratio of a hot plasma that contains a standard mixture of interstellar silicate-graphite dust particles. In § III we derive an observed IRX ratio by comparing IR fluxes from the remnants with existing X-ray fluxes. We determined the IRX ratio for selected remnants which fall into two classes as characterized by their evolutionary state: *the historical or young remnants*, Cas A, Tycho, Kepler, SN 1006, RCW 86, and RCW 103; and the *adiabatic remnants*, IC 443, Puppis A, and the Cygnus Loop. The IR observations and the method used for deriving the IR fluxes from the *IRAS* data are described in § III*a*. From X-ray observations we derive the intrinsic X-ray fluxes in the 0.2–4.0 keV energy band for all remnants. The procedures used to derive these fluxes and to correct them for nonequilibrium ionization effects are described in § III*b*. In § IV we compare the observed to the theoretically derived IRX ratio for the various remnants listed above, and discuss the astrophysical implications of our results. A brief summary of the paper is presented in § V.

II. THE DUST-TO-GAS COOLING AND IRX RATIO OF A DUSTY PLASMA

The relative importance of dust cooling versus gas cooling in a dusty plasma can be expressed as the ratio $\Lambda_d(T)/\Lambda(T)$, where $\Lambda_d(T)$ is the cooling function (ergs cm^3 s^{-1}) of the plasma by means of gas-grain collisions (e.g., Dwek 1987), where T is the plasma temperature, and where $\Lambda(T)$ is the cooling function of the gas by atomic processes (e.g., Raymond, Cox, and Smith 1976). For a given dust composition and dust-to-gas mass ratio, and for a plasma that is in collisional ionization equilibrium, the dust-to-gas cooling ratio is only a function of T. Figure 1 exhibits the value of this ratio versus T (*dashed line*). The IR cooling function $\Lambda_d(T)$ was calculated for a Mathis, Rumpl, and Nordsieck (1977) interstellar dust model in which the grain sizes have been extended to very small sizes. The IR cooling function is directly proportional to the assumed dust-to-gas mass ratio. It is a weak function of the grain size distribution at temperatures below $\sim 10^7$ K and is essentially independent of grain sizes at higher temperatures (see Fig. 4 in Dwek 1987). The largest uncertainties in $\Lambda_d(T)$ arise from those in the fractional energy deposited by electrons into the grains and are always less than $\sim 40\%$. The value of $\Lambda(T)$ was calculated using the latest equilibrium coronal plasma model of Raymond and Smith (1986).

For most temperatures of interest ($\sim 3 \times 10^6$–10^8 K), $\Lambda(T)$ peaks in the soft X-ray regime. Therefore, for comparison with observations, we also calculated the atomic cooling function, $\Lambda(T)$, in the 0.2–4.0 keV energy band. Our choice

of energy band is based on available X-ray data as explained in § III*b*. We define an infrared-to-X-ray cooling ratio, hereafter referred to as the IRX ratio, as:

$$\mathrm{IRX} \equiv \Lambda_d(T)/\Lambda_{0.2-4.0}(T). \quad (1)$$

The IRX ratio is depicted (*solid line*) as a function of gas temperature in Figure 1.

III. THE OBSERVED INFRARED-TO-X-RAY COOLING RATIO

If the dust that gives rise to the IR emission occupies the same volume as the X-ray emitting plasma, then the theoretically calculated IRX ratio should be equal to the ratio between the IR and 0.2–4.0 keV flux from the remnant. As explained in the Introduction, any deviations between the observations and the theoretical IRX ratio will suggest a breakdown in one or more of the assumptions made about the origin of the IR emission.

a) Infrared Observations of Galactic Supernova Remnants

The IR fluxes presented here were obtained from *IRAS* sky maps that were co-added from survey data to obtain high signal-to-noise ratios and spatial resolution. Total uncertainties in the *IRAS* fluxes are ~ 20% for the 100 μm band, and ~ 15% for the 12, 25, and 60 μm bands. Any large-scale gradients present in the field resulting from calibration drifts were removed by imposing a smooth behavior on the median value of points with low signal-to-noise ratio in neighboring scan lines (Young *et al.* 1985).

There are several dust components that are not associated with the remnant that may contribute to the integrated IR flux from the direction of the remnant: (1) the main zodiacal cloud emission; (2) zodiacal dust bands; (3) infrared cirrus; and (4) any Galactic or extragalactic extended or point sources. The main zodiacal emission component (described by Hauser *et al.* 1984) has a flat spatial distribution over the dimensions of all remnants considered here. The contribution of this component to the IR emission was therefore removed from the data by the subtraction of a flat background. The zodiacal dust bands may have spatial structure on a scale of ~ 60′, but were found not to cross any of the remnants. The infrared cirrus, a new component of IR emission discovered by the *IRAS* (Low *et al.* 1984), consists of dust heated by the interstellar radiation field, and exhibits filamentary structure on all scales. Its morphology and color temperature are, however, significantly different from those of a remnant, and a preliminary examination of the maps showed that the contribution of infrared cirrus to the 60 and 100 μm emission from within the remnants is less than about 20%. Extended IR sources are similarly distinguishable from the remnant emission and were found to have a negligible contribution to the flux from the remnant. Point sources, present mostly at 12 and 25 μm, were removed from the maps only if they were prominent, and located within the remnant.

The IR flux from a remnant was obtained by summing up the fluxes in a series of annular rings centered on the radio center of the remnant and extending out to the radio radius of the remnant. This procedure prevented any sources located outside the projected area of the remnant from contributing to the IR emission attributed to the remnant. For most remnants this IR flux is dominated by thermal emission from shock-heated dust. Calculation of other potential IR emission mechanisms, such as synchrotron radiation from accelerated electrons and free-free radiation from ionized species in the optical nebulosities, show them to contribute negligibly to the observed flux. Infrared lines from shocked atoms could provide larger contributions. In Cas A, Dwek *et al.* (1987) showed that line emission constitutes a negligible fraction of the total IR emission. For IC 443, Mufson *et al.* (1986) estimated that line emission may represent as much as 40% of the total IR flux from the remnant. A more recent estimate of the integrated Hα emission from the remnant, which provides the basis for the calculation of the IR line flux, suggests that the line contribution may be significantly smaller than previously thought (Braun 1987*b*). The estimate of Mufson *et al.* (1986) can be used as an upper limit for the sample of remnants reported here, as IC 443 has the most extensive system of optical filaments, where the IR lines would be produced.

The four *IRAS* bands cover the 8–120 μm wavelength regime with an effective bandwidth of ~ 80 μm. We derived total IR fluxes by fitting a single-temperature blackbody modified by a $V^{1.5}$ dust emissivity law to the data. The resulting IR fluxes, attributed to thermal emission from dust in the remnant, are listed in Table 1. Since we did not correct these fluxes for the potential contamination from infrared cirrus and line emission, they may be overestimates by as much as a factor of 2. This accuracy is sufficient for the purpose of this *Letter*. A more accurate assessment of their contribution is, however, pertinent for the detailed modeling of the physical processes that give rise to the IR emission from a remnant.

b) The X-Ray Observations

To construct an observed IRX ratio it is necessary to estimate the intrinsic X-ray flux emitted by each remnant in some standard energy band. Two corrections must therefore be applied to the observed X-ray fluxes: (1) a correction converting all the flux estimates to a common X-ray band; and (2) a correction for the amount of interstellar photoelectric absorption in the various lines of sight to the remnants. Corrections for these effects were made by the following procedure.

We first collected all the available literature on X-ray emission from these remnants. Some remnants had more than one reference with enough information to calculate its intrinsic flux. For these remnants we chose the latest reference, which was usually an observation with the *Einstein Observatory* (Giacconi *et al.* 1979), and made no attempt to combine or reconcile the earlier measurements. Based on this literature we choose the energy band of the HRI instrument[2] of the

[2]Various authors quote different edges for the HRI bandpass; the effective area has a complex shape so the exact choice of "edge" position is somewhat arbitrary. As the HRI has no spectral capability, we assume that all measurements made with the HRI have the same effective bandpass and made no attempt to correct HRI fluxes for the different bandpasses quoted.

TABLE 1

THE INFRARED AND X-RAY PARAMETERS OF SELECTED REMNANTS

SNR (1)	Infrared Flux (10^{-9} ergs cm^{-2}s^{-1}) (2)	T (10^7 K) (3)	N_H (10^{21} cm^{-2}) (4)	0.2–4.0 keV Flux (10^{-10} ergs cm^{-2}s^{-1}) (5)	n_0 (cm^{-3}) (6)	T_s (10^7 K) (7)	η (10^{51} ergs cm^{-6}) (8)	HSC Correction Factor[a] (9)	Observed IRX Ratio[b] (10)
Kepler	1.3	2.0	2.8	3.4	6.0	3.1	11.	2.5	9.6
Tycho	4.1	8.1	3.0	1.7	0.3	40.	0.3	2.5	60.
Cas A	22.	4.6	10.	2.3	11.	2.7	1.2	3.7	350.
SN 1006	< 0.6	0.12, 1.0	1.0	2.9	0.055	28.	0.003	2.0	< 4.1
Puppis A	68.	0.3	4.0	380.	0.1	1.0	0.01	2.9	5.2
IC 443	81.	1.2	6.0	12.	0.2	1.8	0.01	5.4	360.
RCW 86	21.	1.4	0.3	1.9	0.2	4.9	0.004	9.0	990.
RCW 103	< 4.0	0.5	6.0	48.	0.9	0.9	0.04	3.0	< 2.5
Cygnus Loop	79.	0.3	0.4	140.	< 0.1	> 0.3	> 0.015	1.4	7.9

[a] Correction factor to appropriate nonequilibrium ionization (NEI) model from HSC Fig. 18.

[b] The observed IRX ratio is the ratio between the infrared flux (col. [1]) and the "equilibrium" 0.2–4.0 keV flux (col. [5] divided by the HSC correction factor in col. [9]).

NOTES ON INDIVIDUAL REMNANTS.—*Kepler*: Flux, T, N_H from White and Long 1983; NEI parameters from Hughes and Helfand 1985. *Tycho*: *Shell component only*; flux, T, N_H from Seward, Gorenstein, and Tucker, 1983; NEI spectral parameters from Hamilton, Sarazin, and Szymkowiak 1986*b*. *Cas A*: Flux, T, N_H *for shell component only* from Murray *et al.* 1979; NEI parameters *for entire remnant* from Pravdo and Nugent 1983. *SN 1006*: Flux, T, N_H *for entire remnant* from the two-temperature model of Pye *et al.* 1981; NEI spectral parameters *for forward shock only* from Hamilton, Sarazin, and Szymkowiak 1986*a*. *Puppis A*: Flux based on HRI rate in Petre *et al.* 1982 and referenced spectral parameters; NEI parameters from Szymkowiak 1985. *IC 443*: Petre *et al.* 1986; flux, T for hot (shock) component only; NEI parameters are averages over the remnant. *RCW 86*: Flux, T, N_H from Pisarski, Helfand, and Kahn 1984; NEI parameters from Nugent *et al.* 1984. *RCW 103*: All spectral parameters from Nugent *et al.* 1984; flux based on HRI rate from Tuohy and Garmire 1980. *Cygnus Loop*: Flux, T, N_H from Ku *et al.* 1984. NEI parameters from Vedder *et al.* 1986. Joint variations of η and T_s yield an approximately constant correction factor.

Einstein Observatory, nominally from about 0.2 to 4.0 keV, to be our standard band. There were two reasons for this choice. First, we found that flux estimates using this instrument were available for six of our nine objects, so the number of objects requiring a band correction is minimized. Second, the X-ray spectra peak within this band for the range of temperatures likely to be present in these SNRs, and thus we get more of the total flux than if we had chosen a larger, higher energy band, typical of older proportional counter observations. To estimate the 0.2–4.0 keV fluxes for the remnants with quoted fluxes in a different band (IC 443, SN 1006, and the Cygnus Loop) we used the following procedure. From the literature we obtained the value of T, the temperature of the best fitting single temperature equilibrium model, and N_H, the fit value for the amount of interstellar material in the line of sight (columns labeled T and N_H in Table 1). While the plasma in young remnants is most likely not yet in collisional equilibrium, we can make use of these simplified models since we are interested only in how well the model reproduces the observed spectrum, and are not drawing physical conclusions from the parameters. We then determine the normalization parameter that, when multiplying a Raymond-Smith collisional ionization model, gives the quoted flux in the quoted energy band. Then, fixing the normalization parameter and removing the model of the interstellar absorption, we determine the flux of that model in our standard bandpass. The "adjustment" from the values listed in the literature was small, less than ~ 20%. Applying all the above corrections yielded the 0.2–4.0 keV flux at the source which is listed in column (5) of Table 1. In young remnants the ejecta that have been heated by the reverse shock can contribute a large portion of the total X-ray flux. For two remnants of our sample, Cas A and Tycho, the authors of the analyses of the X-ray images identified contributions from the ejecta and from the forward shock. In computing the IRX ratio for these remnants we have used only the X-ray flux arising from the forward shock, as there is no compelling reason to believe that there will be dust in the ejecta (Dwek *et al.* 1987) and we are primarily interested here in comparing the amount of cooling due to dust and gas from shocks in the normal dusty ISM. For the other remnants of our sample, we do not have information to allow us to remove the ejecta component and have used the total X-ray flux in calculating the IRX ratios. For young remnants, such as Kepler and SN 1006, where much of the X-ray flux may arise in ejecta, our estimates of the IRX ratios are therefore probably too small.

The model curve of Figure 1 plots the IRX ratio for dust immersed in a plasma in collisional equilibrium at the temperature given by the abscissa, a condition seldom achieved in adiabatic remnants (Hamilton, Sarazin, and Chevalier 1983, hereafter HSC). To compare our remnant data with the predictions of this simple model, we need to know the proper value of the plasma/shock temperature, and to take into account the fact that the X-ray emission from a plasma not in ionization equilibrium is enhanced over that from an equilibrium plasma. We therefore turn to the more sophisticated nonequilibrium ionization remnant models. These models are characterized by the following set of parameters: n_0, the preshock gas density; T_s, the shock temperature; and $\eta = n_0^2 E_0$, where E_0 is the energy of the explosion. The parameter η is a collisional time scale parameter that characterizes the departure of the plasma from ionization equilibrium (see HSC

for a description of these models and their realm of applicability). Nonequilibrium analyses of X-ray observations were available for all of our remnants, and the model parameters (taken from the references listed in the notes to Table 1) are listed in columns (6)–(8), respectively. The parameters T_s and η determine the multiplicative factor by which the equilibrium X-ray flux from a remnant increases when nonequilibrium ionization is considered. This factor was determined from Figure 18 of HSC and is given, under the label "HSC c.f.", in column (9) of Table 1. The observed X-ray fluxes (col. [5]) are then divided by these correction factors to produce an estimate of the flux the remnant would have if in equilibrium which matches the simple model used to make the theoretical curve of Figure 1. These corrected X-ray fluxes are used with the infrared flux from column (2) to form the IRX ratio of column (10).

IV. ASTROPHYSICAL IMPLICATIONS

a) *Remnant Cooling by Infrared Emission*

The results of Table 1 and Figure 1 show that for all remnants considered here (with the possible exception of SN 1006 and RCW 103) the observed values of the IRX ratio is significantly larger than unity, ranging from ~ 5 in Puppis A, to ~ 1000 in RCW 86. *These results clearly indicate that infrared emission, mostly attributed to gas-grain collisions, is the dominant cooling mechanism in these supernova remnants over large periods of their evolutionary lifetime.*

The comparison of the observed IRX ratios with the theoretical values shows that only the Cygnus Loop and Cas A have observed IRX values that are within a factor of 2–3 of the theoretical one. We consider these remnants to be consistent with the theory, since the dust-to-gas mass ratio can vary by about a factor of 2 in the general ISM, and the calculated value of the IRX ratio is uncertain by a factor of ~ 1.4. This agreement, and the morphological similarities of these remnants at IR (primarily at 60 μm) and X-ray wavelengths, supports the general assumptions made about the origin of the IR emission from these remnants: (1) the IR emission originates from dust that occupies the same volume as the X-ray emitting plasma; (2) the dust is not significantly depleted in the postshock gas relative to the general interstellar medium; and (3) the dust is collisionally heated by the ambient gas.

b) *Deviations from the Theoretical IRX Ratio: Remnant Interaction with the ISM*

For all other remnants the IRX ratio deviates by more than a factor of 3 from its predicted value. The ratio falls significantly below its theoretical value for Puppis A, Kepler, and Tycho. For RCW 103 and SN 1006 we can derive only upper limits on the IRX ratio which fall significantly below the theoretically expected value for these remnants. These deviations suggest that the dust is severely depleted or not well coupled to the gas in these remnants. In Kepler and SN 1006 the low IRX ratio may mostly reflect the absence of dust in the material heated by the reverse shock. Infrared cooling may, however, still be the dominant cooling mechanism in SN 1006, and possibly also in RCW 103. Kepler is located at a distance of about 600 pc above the Galactic plane, which has led to the suggestion that the medium around the remnant is constituted mostly of material that was lost from the presupernova star (White and Long 1983). The IR observations then suggest that very little dust was formed in the ejecta during the presupernova mass loss phase of the progenitor star.

The observed IRX ratio is significantly higher than that predicted for the remnants RCW 86 and IC 443. This, and the fact that these remnants are expanding into an inhomogeneous medium, suggests that a significant fraction of the IR emission is from lines, or does not originate from the X-ray emitting gas. IC 443 has a large number of optical nebulosities, and Dinerstein *et al.* (1986), and Dwek *et al.* (1987) have shown that IR lines from excited atomic species may contribute to the IR emission in the *IRAS* bands. However, even if we assume that as much as 20% of the total IR luminosity is due to line emission, the IRX ratio will still be significantly above that suggested on the basis of the X-ray observations. This may suggest that a significant fraction of the IR flux arises from dust immersed in gas that has cooled below X-ray emitting temperatures. Additionally, a large fraction of the IR emission arises in the region where the IC 443 shock front is encountering a molecular cloud, suggesting that molecular lines may constitute an additional source of emission in the *IRAS* bands.

An overlay of the X-ray and 60 μm emission from RCW 86 shows that a significant fraction of the IR emission originates from a presumably dense region just ahead of the shocked X-ray emitting plasma, in the southwest corner of the remnant. The bulk of the IR emission may therefore be produced by a radiative precursor propagating through this cloud. No IR emission was detected from the northwest, suggesting that in that region the remnant is expanding into a tenuous medium.

c) *Effect on Remnant Evolution*

An important question is if the IR cooling of the remnants will accelerate their evolution compared with the standard evolutionary picture presented, for example, by Cox (1972). The first evolutionary stage of the remnant is the free expansion phase, terminated when enough mass has been swept up to begin decelerating the shock. This is not affected by radiative processes behind the shock. The second stage of remnant evolution, the adiabatic phase, is terminated when about half of the thermal energy of the remnant has been radiated away. The end of this phase is marked by the formation of a dense shell behind the shock and the beginning of the "snowplow" phase of remnant evolution. Enhanced cooling resulting from gas-grain collisions may therefore significantly affect the duration of the adiabatic phase.

The importance of dust cooling depends on the density of the ISM and can be qualitatively assessed in the following way: Consider a remnant with $E_0 = 10^{51}$ ergs expanding into an ISM with $n_0 = 1$ cm^{-3}. The postshock temperature at the end of the adiabatic phase, T_c is about 5×10^5 K, whereas IR emission dominates the cooling of the remnant when $T > 6 \times 10^5$ K (e.g., Fig. 4 in Dwek 1978). Gas-grain colli-

sions will therefore have only a moderate effect on the duration of the adiabatic phase, since most of the thermal energy is lost from the remnant when its volume is largest, i.e., around temperatures of $\sim 6 \times 10^5$ K when IR and atomic cooling are about equally important. At densities of $n_0 = 100$ cm^{-3}, T_c is about 2×10^6 K, so that most of the thermal energy is lost when IR emission dominates the cooling by a large factor. Calculations by Dwek (1981) show that the adiabatic phase is shortened by only $\sim 10\%$ in the former case, and by as much as $\sim 40\%$ in the latter case. At higher densities IR cooling should be more pronounced. However, grain destruction becomes increasingly important as well, resulting in a decrease in the effect of gas-grain collisions on remnant evolution. All adiabatic remnants considered here expand into media with densities < 10 cm^{-3}, so that the IR emission will have a negligible effect on their general evolution.

V. SUMMARY

We calculated the IR-to-X-ray cooling ratio (IRX ratio) from a dusty plasma with a standard interstellar dust-to-gas mass ratio in which the dust particles are collisionally heated by the hot gas. We derived an observed IRX ratio for various remnants from the ratio between their IR and 0.2–4.0 keV fluxes. The remnants included in our analysis, and the results of these calculations are listed in Table 1. The major conclusions of our study are as follows:

1. The observed values of the IRX ratio are larger than unity for most remnants, ranging from 5 for the adiabatic remnant Puppis A, to about 10^3 for RCW 86. Morphological similarities at infrared and X-ray wavelengths, and estimates of the possible contribution of the various mechanisms to the IR emission, suggest that most of the observed IR emission from the remnants can be attributed to thermal emission from dust that is collisionally heated by the shocked plasma. The *IRAS* observations constitute therefore the first observational evidence that gas-grain collisions are the dominant cooling mechanism of the shocked gas in these remnants.

2. A comparison between the theoretical and observed IRX ratio shows that only two of the nine remnants (the Cygnus Loop and Cas A) have IRX ratios within a factor of ~ 3 of the expected value. Variations of this magnitude are consistent with the uncertainties in the calculated IRX ratio, and with the expected magnitude of the variations in the local dust-to-gas mass ratio throughout the ISM.

3. Puppis A, Kepler, Tycho, and SN 1006 have IRX ratios that are significantly smaller than the theoretically predicted value, suggesting that the dust is significantly depleted in the ambient medium into which they are expanding. In addition, the dust may be poorly coupled to the gas in the postshock region. Kepler and SN 1006 are both located high above the Galactic plane, where the dust may well be depleted compared with normal Galactic values.

4. The remnants RCW 86 and IC 443 have IRX ratios that are significantly higher than those predicted by theory. These remnants are expanding into an inhomogeneous medium, suggesting that infrared line emission and/or thermal emission from dust not associated with the X-ray emitting gas may contribute significantly to the observed IR emission in these remnants.

5. The enhanced cooling, over that calculated from atomic transitions only, will not significantly affect the dynamical evolution of the remnants considered here since they expand into relatively low-density ($n_0 < 10$ cm^{-3}) media.

This research was supported under NASA's *IRAS* Data Analysis Program which is funded through the Jet Propulsion Laboratory. We wish to acknowledge the referee for his careful reading and useful suggestions for improvements to the text. We thank Mike Hauser for his comments on an earlier version of the manuscript.

REFERENCES

Arendt, R. G. 1987, private communication.
Braun, R. 1986*a*, *Astr. Ap.*, **164**, 193.
_____. 1986*b*, *Astr. Ap.*, **164**, 208.
_____. 1987*a*, *Astr. Ap.*, **171**, 233.
_____. 1987*b*, private communication.
Burke, J. R., and Silk, J. 1974, *Ap. J.*, **190**, 1.
Cox, D. P. 1972, *Ap. J.*, **178**, 159.
Dalgarno, A., and McCray, R. 1972, *Ann. Rev. Astr. Ap.*, **10**, 375.
Dinerstein, H. L., Lester, D. F., Rank, D. M., Werner, M. W., and Wooden, D. H. 1986, *Ap. J.*, **312**, 314.
Draine, B. T. 1981, *Ap. J.*, **245**, 880.
Dwek, E. 1981, *Ap. J.*, **247**, 614.
_____. 1987, *Ap. J.*, in press.
Dwek, E., Dinerstein, H. L., Gillett, F. C., Hauser, M. G., and Rice, W. L. 1987, *Ap. J.*, **315**, 571.
Giacconi, R., *et al.* 1979, *Ap. J.*, **230**, 540.
Graham, J. R., Evans, A., Albinson, J. S., Bode, M. F., and Meikle, W. P. S. 1987, *Ap. J.*, **319**, 126.
Hamilton, A. J. S., Sarazin, C. L., and Chevalier, R. A. 1983, *Ap. J. Suppl.*, **51**, 115 (HSC).
Hamilton, A. J. S., Sarazin, C. L., and Szymkowiak, A. E. 1986*a*, *Ap. J.*, **300**, 698.
_____. 1986*b*, *Ap. J.*, **300**, 713.
Hauser, M. G., *et al.* 1984, *Ap. J.* (*Letters*), **278**, L15.
Hughes, J. P., and Helfand, D. J. 1985, *Ap. J.*, **291**, 544.
Ku, W. H.-M., Kahn, S. M., Pisarski, R. L., and Long, K. S. 1984, *Ap. J.*, **278**, 615.
Low, F. J., *et al.* 1984, *Ap. J.* (*Letters*), **278**, L19.
Mathis, J. S., Rumpl, W., and Nordsieck, K. H. 1977, *Ap. J.*, **217**, 425.
Mufson, S. L., McCollough, M. L., Dickel, J. R., Petre, R., White, R., and Chevalier, R. 1986, *A.J.*, **92**, 1349.
Murray, S. S., Fabbiano, G., Fabian, A. C., Epstein, A., and Giacconi, R. 1979, *Ap. J.* (*Letters*), **234**, L69.
Nugent, J. J., Pravdo, S. H., Garmire, G. P., Becker, R. H., Tuohy, I. R., and Winkler, P. F. 1984, *Ap. J.*, **284**, 612.
Ostriker, J. P., and Silk, J. 1973, *Ap. J.* (*Letters*), **184**, L113.
Petre, R., Canizares, C. R., Kriss, G. A., and Winkler, P. F. 1982, *Ap. J.*, **258**, 22.
Petre, R., Szymkowiak, A. E., Seward, F. D., and Willingale, R. 1986, *Ap. J.*, submitted.
Pisarski, R. L., Helfand, D. J., and Kahn, S. M. 1984, *Ap. J.*, **277**, 710.
Pravdo, S. H., and Nugent, J. J. 1983, in *IAU Symposium 101, Supernova Remnants and their X-Ray Emission*, ed. J. Danziger and P. Gorenstein (Dordrecht: Reidel), p. 29.
Pye, J. P., Pounds, K. A., Rolf, D. P., Seward, F. D., Smith, A., and Willingale, R. 1981, *M.N.R.A.S.*, **194**, 569.

Raymond, J. C., Cox, D. P., and Smith, B. W. 1976, *Ap. J.*, **204**, 290.
Raymond, J. C., and Smith, B. W. 1986, private communication.
Seward, F., Gorenstein, P., and Tucker, W. 1983, *Ap. J.*, **266**, 287.
Silk, J., and Burke, J. R. 1974, *Ap. J.*, **190**, 11.
Szymkowiak, A. E. 1985, Ph.D. thesis, University of Maryland; also appeared as NASA TM-86169.
Tuohy, I., and Garmire, G. 1980, *Ap. J.* (*Letters*), **239**, L107.
Vedder, P. W., Canizares, C. R., Markert, T. H., and Pradhan, A. K. 1986, *Ap. J.*, **307**, 269.
White, R. L., and Long, K. S. 1983, *Ap. J.*, **264**, 196.
Young, E. T., Neugebauer, G., Kopan, E. L., Benson, R. D., Conrow, T. P., Rice, W. L., and Gregorich, D. T. 1985, preprint.

ELI DWEK: Code 685, NASA/Goddard Space Flight Center, Greenbelt, MD 20771

ROBERT PETRE and ANDREW SZYMKOWIAK: Code 666, NASA/Goddard Space Flight Center, Greenbelt, MD 20771

WALTER RICE: Infrared Processing and Analysis Center 100-22, Caltech, Pasadena, CA 91125